



# Effect of the angle between gas flow direction and electrode on single-chamber SOFC stacks

Yanting Tian<sup>1</sup> · Zhe Lü<sup>2</sup> · Zhihong Wang<sup>2</sup> · Bo Wei<sup>2</sup> · Xiang Guo<sup>1</sup> · Pingping Wu<sup>1</sup>

Received: 7 February 2019 / Revised: 27 March 2019 / Accepted: 28 March 2019 / Published online: 13 April 2019  
© Springer-Verlag GmbH Germany, part of Springer Nature 2019

## Abstract

Single-chamber solid oxide fuel cell (SC-SOFC) stacks with different angles between the gas flow direction and the electrode were fabricated and tested in a diluted methane-oxygen mixture. The gas tubes with separated gas vents were used for transmission of the reactant gasses. Experimental results showed that the performance of the two-cell stack at a gas flow angle ( $\theta$ ) of  $45^\circ$  was greatly enhanced compared with that at  $0$  and  $90^\circ$ . At a furnace temperature of  $700^\circ\text{C}$  and a  $\text{CH}_4/\text{O}_2$  ratio of 2, the maximum output power of the anode-first configuration was  $154\text{ mW}$  at  $\theta = 45^\circ$ , which was 51% higher than that obtained at  $\theta = 90^\circ$ . Additionally, the maximum power of the anode-first stack was higher than that of the cathode-first one at  $\theta = 45^\circ$ , which was contrary to the results obtained at  $\theta = 90^\circ$ . The stack with an angled configuration of  $\theta = 45^\circ$  will generate a more attractive power for portable power applications.

**Keywords** Single-chamber solid oxide fuel cell · Micro-stack · Separated gas supply method · Gas flow angle

## Introduction

Solid oxide fuel cells (SOFCs) have attracted particular attentions recently because of their environmental friendliness, fuel flexibility, and high overall efficiency [1–3]. Fuel-rich gas is transported to the anode and oxygen-rich gas to the cathode in conventional dual-chamber SOFCs. Any mixing of the two reactant gasses is prohibited. The need for gas separation and sealing imposes several challenges on the reliability and long-term stability of these fuel cells. In comparison with the conventional SOFCs, single-chamber SOFCs (SC-SOFCs) are operated in a diluted gas mixture of fuel and oxygen with only one gas chamber [4–6]. The sealing process is thus completely eliminated and the gas-tight electrolytes are non-essential. The operation mechanism of SC-SOFCs is based on the selectivity

properties of the anode and cathode towards the fuel and oxygen mixture [7, 8]. The anode must be catalytically active for partial oxidation of the fuel and electrochemically active for fuel oxidation, whereas the cathode should catalyze the reduction of oxygen, thus generating an electromotive force between the electrodes.

The simple structure of the SC-SOFCs is more flexible for bulky cell designs and stack build-up. Considerable efforts have been devoted to the development of SC-SOFC stacks. Shao et al. [9] proposed a thermally self-sustaining micro-SOFC stack consisting of two cells with an anode-facing-anode configuration. High power output and rapid start-up were demonstrated by using single-chamber operation. The catalytic oxidation reactions supplied sufficient thermal energy to maintain the cells at  $500\text{--}600^\circ\text{C}$ . A micro-stack with two single cells arranged in an anode-facing-cathode configuration was fabricated and operated by Liu et al. [10]. The open-circuit voltage (OCV) of the stack was larger than  $2.0\text{ V}$  at  $700^\circ\text{C}$ , and a maximum power output of about  $371\text{ mW}$  was obtained. For the micro-stack with three cells, a maximum power output of  $282\text{ mW}$  was generated at  $800^\circ\text{C}$  [11]. The cell in the middle place produced a higher power than the others. They found that the heat effect and flow geometry were the main factors in inducing the difference among the cells. A cell-array stack of five anode-supported cells connected in series was also studied [12]. Three single

✉ Yanting Tian  
yanting\_005@163.com

✉ Zhe Lü  
lvzhe@hit.edu.cn

<sup>1</sup> College of Physics and Optoelectronics, Taiyuan University of Technology, Taiyuan 030024, China

<sup>2</sup> Department of Physics, Harbin Institute of Technology, Harbin 150001, China

cells were arranged in the upstream portion and two cells were arranged in the downstream portion. The additional two cells can increase the fuel utilization of the stack. However, the traditional gas supply method severely restricts the formation of a longer stack module in space. The downstream portion of the stack is exposed to the products resulting from fuel oxidation in the upstream portion of the stack, which will lead to a performance drop by reforming the gasses over the electrodes. The stack design plays a significant role with respect to cell performance. The gas flow geometry should allow uniform, continuous flow of the fuel-air mixture to anode and cathode [4].

In our previous study of SC-SOFC micro-stack, a novel gas supply method with separated gas vents in the gas tubes was proposed to ensure the identical gas distribution over the electrodes [13]. Two gas tubes flanking the stacks were used as gas channels of methane and oxygen for anodes and cathodes, respectively. An OCV of 1.8 V and a maximum power output of 276 mW were produced by a two-cell stack. The separated gas supply mode is more flexible to form an enlarged stack module in three-dimensional space. A scaled-up stack with six cells in series generated an OCV of 6.4 V and a maximum power output of 8.18 W by using the separated gas supply method with two gas tubes [14]. Additionally, the effect of the separated gas supply mode and the traditional gas supply method on the performance of the micro-stack and single cells were compared [15]. Results showed that the single cells could obtain a uniform OCV and power output by using the

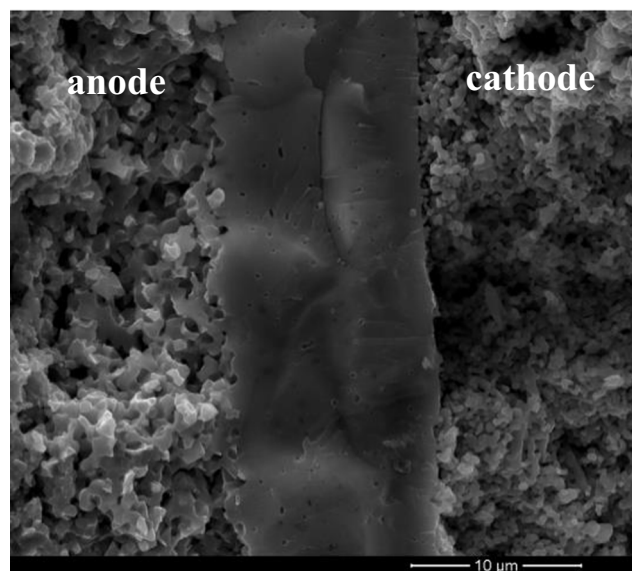


Fig. 2 SEM micrograph of the cell structure after reduction of the anode

separated gas supply method. The tubes with evenly arranged vents created a uniform mixing and distribution of the gas mixture over the single cells. For the traditional gas supply method, the cells at the outlet position yielded inferior performance compared with that of the inlet cells. Eventually, a higher performance was produced by the separated gas supply method.

In this study, we are thus continuing our investigation of SC-SOFC micro-stacks by using the separated gas supply

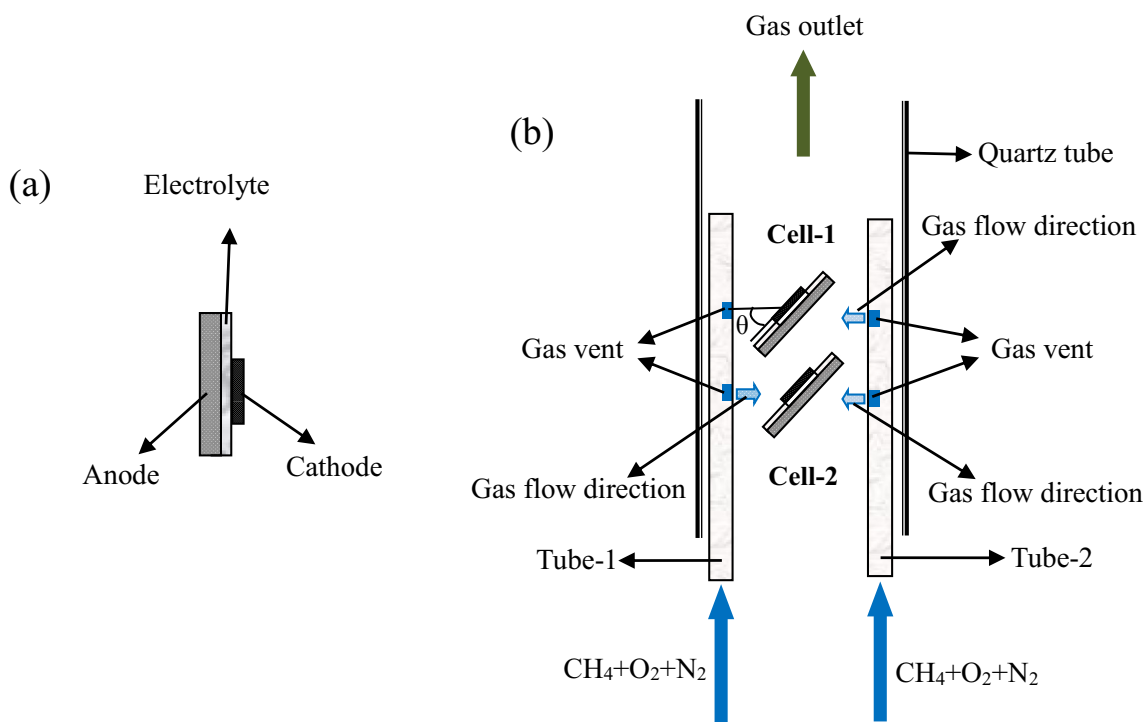


Fig. 1 Schematic illustrations of the cell configuration and the stack: **a** single cell and **b** perspective view of the stack. Performed with the drawing function of MSOffice

method. The performance of the stacks with different configurations was investigated at various fuel-to-oxygen ratios. The influence of the angle between the gas flow direction and the electrode on the performance of the stacks and the single cells was evaluated and analyzed in details.

### Experimental

The single cells were purchased from Ningbo SOFCMAN Energy Technology Co., Ltd. A conventional 50 wt% NiO/50 wt% yttria-stabilized zirconia (YSZ) anode was fabricated using tape casting method as the support of the SOFC. The YSZ electrolyte films with a thickness of 10  $\mu\text{m}$  were prepared by a spraying method.  $(\text{La}_{0.75}\text{Sr}_{0.25})_{0.95}\text{MnO}_3$  (LSM) was then coated onto the YSZ films as the cathode. Figure 1 a shows the schematic diagram of the cell configuration. The size of the cells was  $1 \times 1 \text{ cm}^2$ , and the active cathode area was  $0.7 \times 0.7 \text{ cm}^2$ . NiO in anode substrate was reduced to metallic Ni at 700  $^\circ\text{C}$  in hydrogen atmosphere for about 2 h before assembling to avoid the reduction of the cathodes [16].

The schematic diagram of the two-cell stack is shown in Fig. 1 b. Two half-open ceramic tubes, marked as Tube-1 and

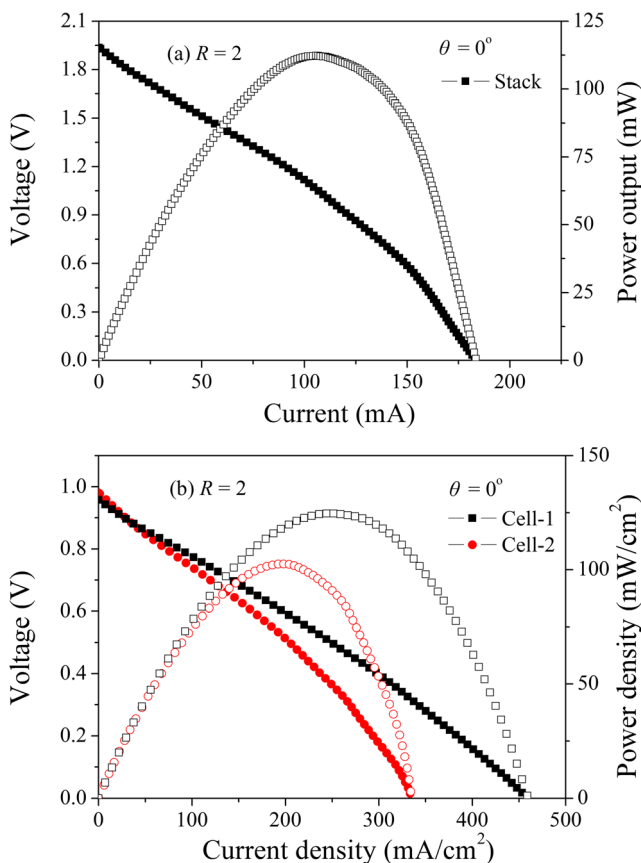


**Fig. 3** The *I-V* and *I-P* curves of the stack and the single cells at  $R = 2$  and  $\theta = 0^\circ$ : **a** stack and **b** single cells. Performed with the graphic program of Origin 8.0

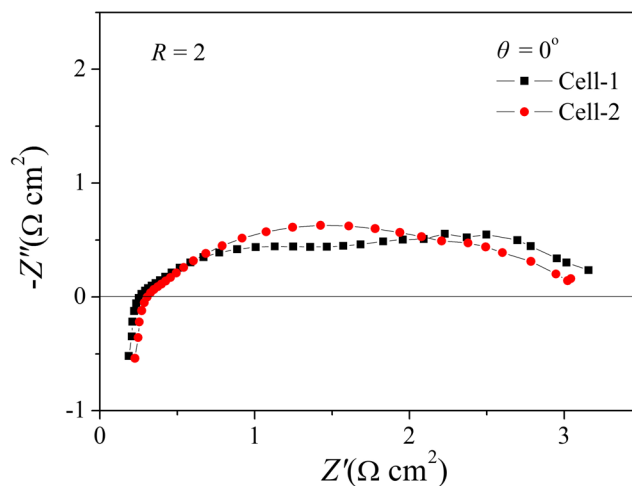


**Fig. 4** Impedance spectra of the single cells at  $R = 2$  and  $\theta = 0^\circ$ . Performed with the graphic program of Origin 8.0

Tube-2, were used to transport the reactant gasses consisting of nitrogen, methane, and oxygen. Each of the tube had an inner diameter of 2 mm and an outer diameter of 3.4 mm. Small gas vents were arranged at the side of the gas tubes for the transport of the gas mixture to the electrodes. Both the width and the depth of the gas inlets were 1 mm. Gas flow directions of the gas vents were shown in Fig. 1 b. The angle between the gas flow direction and the electrode was indicated as  $\theta$ . For a certain angle, the two gas tubes were switched by a ball valve during the testing process. The two cells in the stack were connected in serial by silver wires. Silver paste was coated on the electrode surfaces for current collection and silver wires connection.

The stacks were assembled in a quartz tube with an open end. The inner and outer diameters of the quartz tube were 25 and 30 mm, respectively. The flow rates of nitrogen, methane, and oxygen were controlled by mass flow controllers (MFCs, D08-4D/2M, Seven-Star Huachuang, China). Electrochemical properties of the stacks and single cells were measured by a BiStat potentiostat (VSP, Bio-logic SAS) using

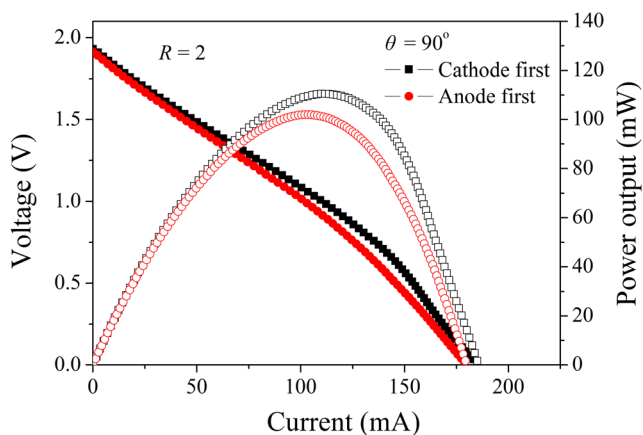


**Fig. 5** The *I-V* and *I-P* curves of the stack at  $R = 2$  and  $\theta = 90^\circ$ . Performed with the graphic program of Origin 8.0

**Table 1** Effect of methane-oxygen ratio on the output performance of the stacks at  $\theta = 0^\circ$  and  $\theta = 90^\circ$ 

700 °C, N <sub>2</sub> = 200 sccm		R = 1	R = 1.5	R = 2
$\theta = 0^\circ$	OCV (V)	1.79	1.86	1.93
Parallel	Maximum power (mW)	85	107	112
$\theta = 90^\circ$	OCV (V)	1.81	1.86	1.93
Cathode-first configuration	Maximum power (mW)	87.8	109	110
$\theta = 90^\circ$	OCV (V)	1.76	1.81	1.91
Anode-first configuration	Maximum power (mW)	77	102	102

the four-terminal method at a furnace temperature of 700 °C. The voltage ramp rate used with the potentiostat was 20 mV/s. The impedance spectra were measured under open-circuit condition from 0.1 Hz to 91 kHz with a signal amplitude of 10 mV.

## Results and discussion

SEM image of the cell structure after reduction of the anode is shown in Fig. 2. The YSZ electrolyte film was uniform and dense enough with a thickness of approximately 10  $\mu\text{m}$  and adhered well to both the porous anode and cathode layers without showing any cracking or delamination, indicating a good match between the electrolyte and the electrodes. The thicknesses of the anode and cathode were about 400 and 25  $\mu\text{m}$ , respectively. The pores in the anode substrate were caused by the burnout of the binder. Also, the reduction of nickel oxide to nickel can increase both the gas-transport path and the three-phase boundary for reaction. The porosity of the anode was 31% and the pore size was 0.5–1.1  $\mu\text{m}$ . For pure cathode, LSM particles were well-contacted and these grains were homogeneous with a particle size of about 0.4  $\mu\text{m}$ . The pore size of the cathode was obviously decreased compared with that of the anode, which was about 0.2–0.6  $\mu\text{m}$ . The porosity of the cathode was 27%.

The performance of the stacks operated under different gas flow angles ( $\theta$ ) was tested in CH<sub>4</sub>-O<sub>2</sub>-N<sub>2</sub> mixtures at 700 °C. Figure 3 shows the current-voltage (*I*-*V*) and current-power (*I*-*P*) curves of the stack and the single cells at  $\theta = 0^\circ$  for the CH<sub>4</sub>/O<sub>2</sub> ratio (*R*) of 2 using Tube-1 as the gas transmission pipeline. The flow rate of N<sub>2</sub> was fixed at 200 sccm and the total flow rate of CH<sub>4</sub> and O<sub>2</sub> was 200 sccm. The stack owned a parallel configuration at  $\theta = 0^\circ$  where the gas flow direction was parallel to the electrode surface. The OCV of the stack was 1.93 V and the maximum power output was 112 mW. The performance of Cell-1 was higher than that of Cell-2. According to Liu et al. [17], the cell whose cathode was located between the two cells showed lower performance due to the insufficient reactive gas for the cathode.

The AC impedance spectra of the single cells measured under open-circuit voltage condition are shown in Fig. 4.

The semicircle at higher frequency is mainly attributed to the charge-transfer polarization of the cathode and the one at a lower frequency is mainly due to the gas dissociative adsorption and/or surface diffusion resistance of the anode, as discussed in the previous study [18]. As can be seen, the high-frequency semicircle of Cell-2 was much higher than that of Cell-1, indicating that the cathode faced the inner side of the stack was distinctly influenced by the gas flow geometry. The gas composition was modified by catalytic oxidation over the anode of Cell-1, which resulted in the decrease of oxygen content at the cathode of Cell-2. The ohmic resistance, which was determined by the actual temperature of the cells [19], also showed a small difference between the two cells. The lower ohmic resistance of Cell-1 presented a direct evidence of its higher temperature. Also, the low-frequency semicircle of Cell-1 was higher than that of Cell-2. The anode of Cell-1 was located in the middle of the stack, which was conducive to heat accumulation but unfavorable to gas diffusion for the anode.

Figure 5 shows the *I*-*V* and *I*-*P* curves of the stack at  $\theta = 90^\circ$  for the CH<sub>4</sub>/O<sub>2</sub> ratio of 2. The stack owned a cathode-first configuration when Tube-1 was used as the gas transmission pipeline. The gas flow direction was perpendicular to the cathodes of the cells. The gas mixture first reached the cathodes for the dissociative adsorption of oxygen and then the remaining gas diffused to the anodes to participate in the reaction.

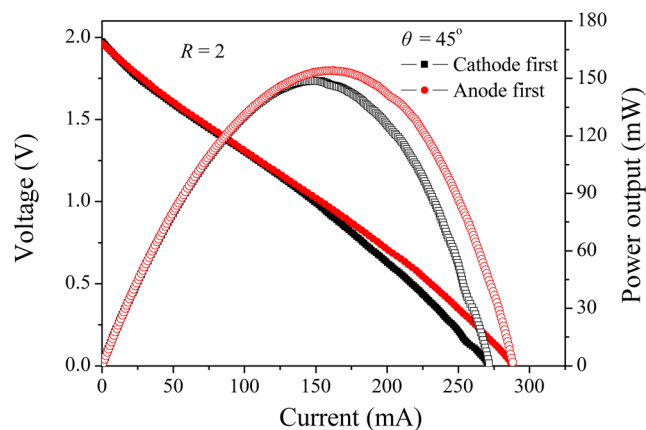


**Fig. 6** The *I*-*V* and *I*-*P* curves of the stack at  $R = 2$  and  $\theta = 45^\circ$ . Performed with the graphic program of Origin 8.0

**Table 2** Effect of methane-oxygen ratio on OCV and maximum power of the stack at  $\theta = 45^\circ$

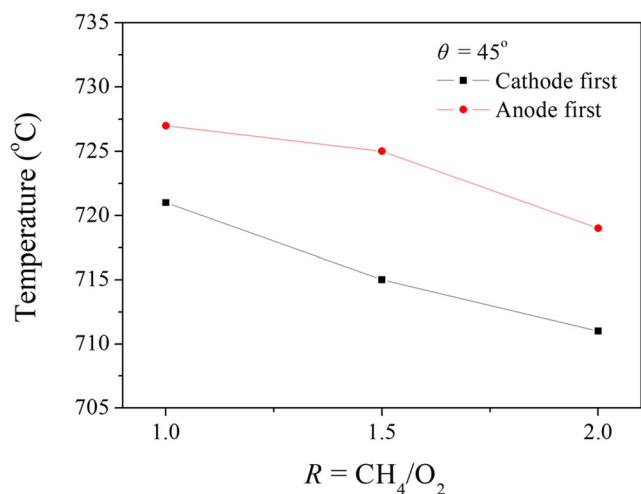
700 °C, N <sub>2</sub> = 200 sccm		R = 1	R = 1.5	R = 2
$\theta = 45^\circ$	OCV (V)	1.84	1.96	1.97
Cathode-first configuration	Maximum power (mW)	131	143	148
$\theta = 45^\circ$	OCV (V)	1.82	1.94	1.96
Anode-first configuration	Maximum power (mW)	143	152	154

Conversely, the stack owned an anode-first configuration when Tube-2 was used. The gas mixture reached the anodes firstly and the gas flow direction was perpendicular to the anodes. The stack with cathode-first configuration achieved an OCV of 1.93 V and a maximum power of 110 mW. The anode-first configuration had a lower output power of 102 mW. Table 1 shows the effect of methane-oxygen ratio on OCV and maximum power of the stacks at  $\theta = 0^\circ$  and  $\theta = 90^\circ$ . The oxygen concentration gradient across the cells showed a strong dependence on the fuel-oxygen ratio. Both OCV and maximum power of the stacks increased with the methane-oxygen ratio. The parallel and the cathode-first configurations achieved almost the same performance while the OCV and maximum power of the anode-first stack were

slightly decreased. Stefan et al. [20] presented similar results using an electrolyte-supported cell in propane-air mixtures. The lower performance obtained in the anode-first configuration was due to the catalytic activity of the anode for the fuel oxidation, which promotes oxygen consumption before the gas mixture reaches the cathode.

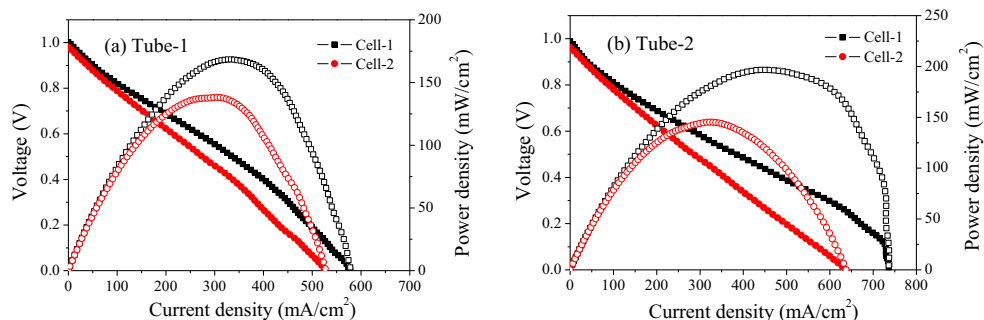
According to the operation mechanism of SC-SOFCs, the anode and cathode have different catalytic activities towards the fuel-oxygen mixture. The relative positioning of the electrodes in regard to the incoming gas should be optimized for both electrodes. Therefore, an angle of  $45^\circ$  between the gas flow direction and the electrode was proposed. Figure 6 shows the *I-V* and *I-P* curves of the stacks at the gas flow angle of  $45^\circ$ . The performance of the stack was obviously improved compared with that at  $\theta = 0^\circ$  and  $\theta = 90^\circ$ . Both the anode and cathode of the cells could obtain reaction gasses expeditiously under the angled configuration. When  $\theta = 90^\circ$ , although it was beneficial to the electrodes directly relative to the gas flow, it was not conducive to the performance of the electrodes on the opposite side of the gas vents. While at  $\theta = 45^\circ$ , the gas mixture flowed through the two cells, which could provide reaction gasses for both of the adjacent electrodes. Compared with the parallel configuration at  $\theta = 0^\circ$ , the angle between the gas flow direction and the electrode could increase the residence time of the reaction gasses on the surface of the electrodes, which made the reaction gasses of the electrodes more abundant. The gas flow angle of  $45^\circ$  was also helpful to heat accumulation around the cells. As a result, the anode-first configuration obtained a maximum power of 154 mW at  $\theta = 45^\circ$ , which was 51% higher than that at  $\theta = 90^\circ$ .

The performances of the stack using Tube-1 and Tube-2 for gas transmission were also different at  $\theta = 45^\circ$ . The gas mixture first reached the cathodes when Tube-1 was used.



**Fig. 7** The temperature of the stack at  $\theta = 45^\circ$  with various  $\text{CH}_4/\text{O}_2$  ratios. Performed with the graphic program of Origin 8.0

**Fig. 8** The *I-V* and *I-P* curves of the single cells at  $R = 2$  and  $\theta = 45^\circ$ : **a** cathode-first configuration and **b** anode-first configuration. Performed with the graphic program of Origin 8.0





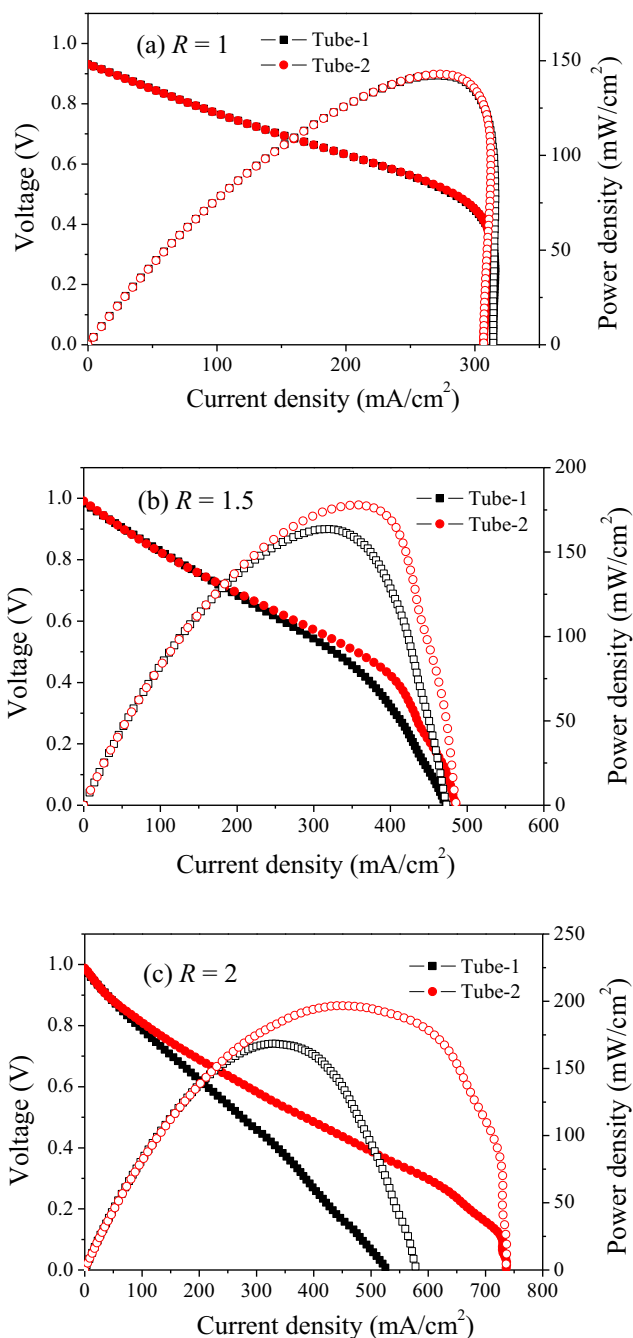
Therefore, sufficient reaction gas could be provided for the cathodes. Meanwhile, the gas mixture reached the anodes firstly when Tube-2 was used. The downstream cathodes were exposed to the gas composition modified by fuel oxidation of the upstream anodes. The two configurations had different reaction processes; therefore, different cell performances were obtained. Table 2 shows the effect of methane-oxygen ratio on OCV and maximum power of the stack at  $\theta = 45^\circ$ . The OCV of the stack was apparently higher than that at  $\theta = 0^\circ$  and  $\theta = 90^\circ$ . Both the OCV and maximum power increased with the increasing gas flow ratio. The cathode-first stack showed a higher OCV than the anode-first configuration. Figure 7 shows the actual temperature of the stack at  $\theta = 45^\circ$  with various  $\text{CH}_4/\text{O}_2$  ratios. The temperature of the anode-first configuration was relatively high, which was beneficial to the cell performance. As a result, the maximum power of the anode-first stack was higher than that of the cathode-first one, as shown in Table 2, which was opposite to the experimental results obtained at  $\theta = 90^\circ$ .

Figure 8 shows the  $I$ - $V$  and  $I$ - $P$  curves of the single cells at  $\theta = 45^\circ$  and  $R = 2$ . The OCV and maximum power density of Cell-1 were higher than that of Cell-2 under the two configurations. The same to the parallel configuration at  $\theta = 0^\circ$ , the oxygen consumption over the anode would affect the performance of the cathode located between the two cells. Results showed less diversity between the two cells of the cathode-first configuration than that of the anode-first configuration. In the anode-first stack, the gas mixture first reached the anode of Cell-1 for fuel oxidation, then the remaining gas diffused to the cathode of Cell-2. Therefore, a stronger influence of the gas flow geometry on the performance of Cell-2 existed. The performances of the single cells of the anode-first stack were higher than that of the cathode-first one, which was caused by the exothermic reaction over the anodes and the effect of gas flow geometry on heat accumulation.

Figure 9 shows the performance of Cell-1 using different gas tubes with various gas flow ratios. The  $I$ - $V$  and  $I$ - $P$  curves of Cell-1 with different configurations were well coincident at  $R = 1$ . However, serious concentration polarization was observed at high current density, because, with increased oxygen concentration, more non-electrochemical active products ( $\text{CO}_2$  and  $\text{H}_2\text{O}$ ) are generated from the complete oxidation reaction, which are deleterious to the electrochemical oxidations of  $\text{H}_2$  and  $\text{CO}$ . The concentration overpotential at the high current part severely limits the output performance of the cell. With the increase of the fuel-oxygen ratio, the cell performances of both the configurations were improved. The catalytic reaction of methane partial oxidation produces  $\text{H}_2$  and  $\text{CO}$ , which are effective electrochemical reaction gasses. The performance diversity of Cell-1 among the different configurations was becoming obvious with the increasing gas flow ratio. The same tendency was observed in the performance of Cell-2 at  $650^\circ\text{C}$  (Fig. S1). The methane-oxygen

ratio of 2 is the stoichiometric value for the partial oxidation of methane. With the partial oxidation reaction becoming the dominant reaction at  $R = 2$ , the performance of the cells with the anode-first configuration was obviously higher than that of the cathode-first configuration.

The residence time of the reaction gas on the electrode surface can be increased when the gas flow direction is at an angle with the electrode. The heat released from partial oxidation of methane could also be used more rationally. Besides,



**Fig. 9** The  $I$ - $V$  and  $I$ - $P$  curves of Cell-1 with various  $\text{CH}_4/\text{O}_2$  ratios: **a**  $R = 1$ , **b**  $R = 1.5$ , and **c**  $R = 2$ . Performed with the graphic program of Origin 8.0

both of the adjacent electrodes could obtain reaction gasses expeditiously. As a result, the output performance of the angled stack is much better than that of the parallel and vertical configurations. Also, the traditional gas supply method severely restricts the formation of a longer stack module in space, where the downstream portion of the stack is exposed to by-products resulting from fuel oxidation in the upstream portion of the stack. The separated gas supply method offers greater potential for portable power generation. It is expected to further improve the output performance of the SC-SOFCs with more cells by using the angled configuration.

## Conclusion

Micro-stacks consisted of two cells were fabricated and operated under single-chamber conditions. A novel gas supply method with separated gas vents in the gas tubes was used for the gas transmission. The influence of the angle between the direction of the gas flow and the surface of the electrodes on the performance of the stacks was investigated in details. The stack at  $\theta = 45^\circ$  showed remarkably enhanced OCV and output power than that at  $\theta = 0^\circ$  and  $\theta = 90^\circ$ . The maximum power of the anode-first stack at  $\theta = 45^\circ$  was higher than that of the cathode-first configuration, which was contrary to the results obtained at  $\theta = 90^\circ$ . The micro-stack with an angled configuration is helpful to increase the residence time of the reaction gas on the electrode surface and also beneficial to heat accumulation around the cells.

**Funding** This work was supported by the National Natural Science Foundation of China (Nos. 51602213, 11604236 and 61575139) and the Youth Foundation of the Taiyuan University of Technology (No. 2015QN071).

## Compliance with ethical standards

**Conflict of interest** The authors declare that they have no conflict of interest.

## References

1. Yang Q, Chen J, Sun CW, Chen LQ (2016) Direct operation of methane fueled solid oxide fuel cells with Ni cermet anode via Sn modification. *Int J Hydrog Energy* 41(26):11391–11398
2. Zhang CM, Zheng Y, Ran R, Shao ZP, Jin WQ, Xu NP, Ahn J (2008) Initialization of a methane-fueled single-chamber solid-oxide fuel cell with NiO + SDC anode and BSCF + SDC cathode. *J Power Sources* 179(2):640–648
3. Chen KF, Tian YT, Lü Z, Ai N, Huang XQ, Su WH (2009) Behavior of 3 mol% yttria-stabilized tetragonal zirconia polycrystal film prepared by slurry spin coating. *J Power Sources* 186(1):128–132

4. Kuhn M, Napporn TW (2010) Single-chamber solid oxide fuel cell technology—from its origins to today’s state of the art. *Energies* 3(1):57–134
5. Napporn TW, Jacques-Bédard X, Morin F, Meunier M (2004) Operating conditions of a single-chamber SOFC. *J Electrochem Soc* 151(12):2088–2094
6. Shao ZP, Mederos J, Chueh WC, Haile SM (2006) High power-density single-chamber fuel cells operated on methane. *J Power Sources* 162(1):589–596
7. Yano M, Tomita A, Sano M, Hibino T (2007) Recent advances in single-chamber solid oxide fuel cells: a review. *Solid State Ionics* 177(39–40):3351–3359
8. Riess I (2008) On the single chamber solid oxide fuel cells. *J Power Sources* 175(1):325–337
9. Shao ZP, Haile SM, Ahn J, Ronney PD, Zhan ZL, Barnett SA (2005) A thermally self-sustained micro solid-oxide fuel-cell stack with high power density. *Nature* 435(7043):795–798
10. Liu ML, Lü Z, Wei B, Zhu RB, Huang XQ, Chen KF, Ai G, Su WH (2007) Anode-supported micro-SOFC stacks operated under single-chamber conditions. *J Electrochem Soc* 154(6):588–592
11. Liu ML, Lü Z, Wei B, Huang XQ, Zhang YH, Su WH (2010) Effects of the single chamber SOFC stack configuration on the performance of the single cells. *Solid State Ionics* 181(19–20):939–942
12. Liu ML, Lü Z, Wei B, Huang XQ, Chen KF, Su WH (2009) A novel cell-array design for single chamber SOFC microstack. *Fuel Cells* 9(5):717–721
13. Tian YT, Lü Z, Wei B, Wang ZH, Liu ML, Li WY, Huang XQ, Su WH (2011) A non-sealed solid oxide fuel cell micro-stack with two gas channels. *Int J Hydrog Energy* 36(12):7251–7256
14. Tian Y, Lü Z, Wei B, Zhu X, Li W, Wang Z, Pan W, Su W (2012) Evaluation of a non-sealed solid oxide fuel cell stack with cells embedded in plane configuration. *Fuel Cells* 12(4):523–529
15. Tian YT, Lü Z, Liu ML, Zhu XB, Wei B, Zhang YH, Huang XQ, Su WH (2013) Effect of gas supply method on the performance of the single-chamber SOFC micro-stack and the single cells. *J Solid State Electrochem* 17(1):269–275
16. Wei B, Lü Z, Huang XQ, Liu ML, Jia DC, Su WH (2009) A novel design of single-chamber SOFC micro-stack operated in methane-oxygen mixture. *Electrochem Commun* 11(2):347–350
17. Liu ML, Lü Z, Wei B, Huang XQ, Chen KF, Su WH (2009) Effect of the cell distance on the cathode in single chamber SOFC short stack. *J Electrochem Soc* 156(10):1253–1256
18. Jasinski P, Suzuki T, Dogan F, Anderson HU (2004) Impedance spectroscopy of single chamber SOFC. *Solid State Ionics* 175(1–4):35–38
19. Morel B, Roberge R, Savoie S, Napporn TW, Meunier M (2007) Catalytic activity and performance of LSM cathode materials in single chamber SOFC. *Appl Catal A-Gen* 323:181–187
20. Stefan IC, Jacobson CP, Visco SJ, De Jonghe LC (2004) Single chamber fuel cells: flow geometry, rate, and composition considerations. *Electrochem Solid-State Lett* 7(7):198–200

**Publisher’s note** Springer Nature remains neutral with regard to jurisdictional claims in published maps and institutional affiliations.